

Simple Designs of Fractional-Order Shelving Filters for Acoustic Systems

Alexandros Pagidas and Costas Psychalinos
Physics Department, Electronics Laboratory
University of Patras
 Rio Patras, Greece
 up1055708@upnet.gr; cpsychal@upatras.gr

Abstract—A novel generalized structure capable for implementing fractional-order shelving filters is presented in this work. This is achieved by forming the realized transfer function as a ratio of two impedances, where the fractional-order one is approximated by a suitable tool. The provided simulation results confirm the validity of the proposed concept.

Index Terms—fractional-order filters, fractional-order capacitors, fractional-order impedances, shelving filters, acoustic applications

I. INTRODUCTION

Shelving filters offer the special characteristic of not completely removing the out-of-band content of a signal, as the standard filter structures perform [1]. They perform a boost or attenuation of a specific band and, according to the location of this band, they fall into the following main categories: a) low-pass filters, which boost or attenuate the low end of the frequency spectrum, and b) high-pass, which boost or attenuate the high end of the frequency spectrum [2]–[7]. According to [8], an important parameter for improving the listening experience is the slope of the boost/attenuation gradient in the transition between the two bands which must be less than of that offered by the conventional integer-order filters. Following this, the fractional-order filtering is an attractive candidate for implementing shelving filters and this is originated from the fact that they offer fine adjustment of slope of the transition, through the order of the filter [9]. Fractional-order shelving filters have been presented in [10], [11]. Although the scheme in [10] is attractive in the sense that it offers electronic adjustment capability of the filter characteristics, it suffers from the increased circuit complexity. The solution published in [11] is simpler, at the expense of losing the electronic tunability.

In the present work, a novel scheme for implementing fractional-order shelving filters is introduced, which offer reduced circuit complexity with regards to that in [11]. This is achieved through the utilization of the concept of the driving impedance, in order to implement the required transfer function. This work is organized as follows: a brief theory of the fractional-order shelving filters is given in Section II, while the proposed implementation is presented in Section III. The simulation results, which support the introduced material, are provided in Section IV.

II. FRACTIONAL-ORDER SHELIVING FILTERS

The transfer function of a low-pass shelving filter, with the low and high frequency gains being G_{max} and G_{min} , respectively, is given by (1)

$$H_{LP}(s) = \sqrt{G_{max}G_{min}} \cdot \frac{\tau s + \sqrt{\frac{G_{max}}{G_{min}}}}{\sqrt{\frac{G_{max}}{G_{min}}\tau s + 1}}. \quad (1)$$

The pole and zero frequencies of (1) are located in equal distance around the characteristic frequency $\omega_0 = 1/\tau$, determined by (2)

$$\omega_P = \omega_0 \cdot \left(\sqrt{\frac{G_{max}}{G_{min}}} \right)^{-1} \quad \omega_Z = \omega_0 \sqrt{\frac{G_{max}}{G_{min}}}, \quad (2)$$

making ω_0 to be the geometric mean of these frequencies (i.e., $\omega_0 = \sqrt{\omega_P \cdot \omega_Z}$), and it is usually mentioned as center frequency.

Setting $s = j\omega$ in (1), the derived expression for the magnitude response is

$$|H_{LP}(\omega)| = (G_{max}G_{min})^{1/2} \cdot \left[\frac{(\omega\tau)^2 + \frac{G_{max}}{G_{min}}}{\frac{G_{max}}{G_{min}}(\omega\tau)^2 + 1} \right]^{1/2}. \quad (3)$$

The gain at the frequency ω_0 is equal to $\sqrt{G_{max}G_{min}}$ and, therefore, is the (geometric) mean of the characteristic gains of the filter. Considering (2), it is derived that the pole and zero relative distance is determined by the ratio of the characteristic gains of the filter. Owing to the fact that the pole and zero locations frequencies are equal to the low (ω_L) and high (ω_H) cutoff frequencies, the slope of the transition between the two bands is also determined by the aforementioned ratio.

The transfer function of a low-pass fractional-order ($0 < \alpha < 1$) shelving filter, is that given by (4)

$$H_{LP}(s) = \sqrt{G_{max}G_{min}} \cdot \frac{(\tau s)^\alpha + \sqrt{\frac{G_{max}}{G_{min}}}}{\sqrt{\frac{G_{max}}{G_{min}}(\tau s)^\alpha + 1}}. \quad (4)$$

The pole and zero frequencies are still equally spaced around ω_0 , and their exact location is given by the expressions in (5)

$$\omega_P = \omega_0 \left(\sqrt{\frac{G_{max}}{G_{min}}} \right)^{-\frac{1}{\alpha}} \quad \omega_Z = \omega_0 \left(\sqrt{\frac{G_{max}}{G_{min}}} \right)^{\frac{1}{\alpha}}. \quad (5)$$

According to (5), the extra degree of freedom (i.e., the order of the filter) offers the capability of adjusting the location of the pole and zero, without disturbing the characteristic gains of the filter.

The low (ω_L) and high (ω_H) cutoff frequencies will be determined according to the following expressions

$$\omega_L = \omega_P \cdot \left[\sqrt{1 + \cos^2 \left(\frac{\alpha\pi}{2} \right)} - \cos \left(\frac{\alpha\pi}{2} \right) \right]^{1/\alpha}, \quad (6a)$$

$$\omega_H = \omega_Z \cdot \left[\sqrt{1 + \cos^2 \left(\frac{\alpha\pi}{2} \right)} + \cos \left(\frac{\alpha\pi}{2} \right) \right]^{1/\alpha}. \quad (6b)$$

The slope of the transition between the two bands can be adjusted through the order of the filter and, therefore, a more precision control of the transition between the two bands is achieved than that achieved by the integer-order filter.

In the case of a fractional-order high-pass filter, with its transfer function given by (7)

$$H_{HP}(s) = \sqrt{G_{max}G_{min}} \cdot \frac{\sqrt{\frac{G_{max}}{G_{min}}} (\tau s)^\alpha + 1}{(\tau s)^\alpha + \sqrt{\frac{G_{max}}{G_{min}}}}, \quad (7)$$

the zero and pole have interchanged their locations with regards to the center frequency, compared to those established by the corresponding low-pass filter. This is described by the expressions in (8)

$$\omega_P = \omega_0 \left(\sqrt{\frac{G_{max}}{G_{min}}} \right)^{\frac{1}{\alpha}} \quad \omega_Z = \omega_0 \left(\sqrt{\frac{G_{max}}{G_{min}}} \right)^{-\frac{1}{\alpha}}. \quad (8)$$

The associated cut-off frequencies are given by (9a)–(9b)

$$\omega_L = \omega_Z \cdot \left[\sqrt{1 + \cos^2 \left(\frac{\alpha\pi}{2} \right)} - \cos \left(\frac{\alpha\pi}{2} \right) \right]^{-1/\alpha}, \quad (9a)$$

$$\omega_H = \omega_P \cdot \left[\sqrt{1 + \cos^2 \left(\frac{\alpha\pi}{2} \right)} + \cos \left(\frac{\alpha\pi}{2} \right) \right]^{-1/\alpha}. \quad (9b)$$

The benefit of the orthogonal adjustment of the slope of the transition between the two bands is still offered, with its value being the opposite one of that realized by the low-pass filter. In order to facilitate the reader, let us consider fractional-order filters with $\{G_{max}, G_{min}\}$ being equal to $\{10, 1\}$ in the case of low-pass and $\{1, 10\}$ in the case of high pass filter, and $f_0 = 0.5 \text{ kHz}$. Their most important frequency characteristics, as well as of their integer-order counterparts, are summarized in Table I, where it is readily obtained the flexibility offered by the fractional-order filtering.

III. IMPLEMENTATION OF FRACTIONAL-ORDER SHELIVING FILTERS

A typical implementation of a fractional-order low-pass shelving filter, using an operational amplifier (op-amp) as active element, is demonstrated in Fig. 1. Taking into account that the impedance of a fractional-order capacitor is given by the formula: $Z = 1/C_\alpha s^\alpha$, with $0 < \alpha < 1$ being the order

TABLE I
COMPARISON OF THE FREQUENCY CHARACTERISTICS OF FRACTIONAL AND INTEGER-ORDER SHELIVING FILTERS.

Parameter	Integer-order	FO-LP filter ^a		
		0.7	0.8	0.9
f_P (Hz)	158.11	96.53	118.57	139.13
f_Z (kHz)	1.58	2.59	2.11	1.79
f_L (Hz)	159.72	58.63	88.16	122.3
f_H (kHz)	1.56	4.26	2.84	2.04
slope (dB/dec)	-20.18	-10.74	-13.27	-16.35

^aIn the case of high-pass filter $f_P \leftrightarrow f_Z$, $f_L \leftrightarrow f_H$, and slope \leftrightarrow -slope.

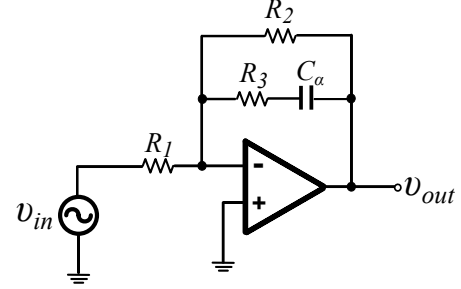


Fig. 1. Fractional-order low-pass shelving filter, implemented using an op-amp as active element.

and C_α being the pseudo-capacitance in $F \cdot s^{\alpha-1}$, the realized transfer function is given by (10)

$$H(s) = -\frac{R_2}{R_1} \frac{R_3 C_\alpha s^\alpha + 1}{(R_2 + R_3) C_\alpha s^\alpha + 1}. \quad (10)$$

Equalizing the coefficients of (4) and (10), the derived design equations are summarized in (11a)–(11c)

$$R_2 = G_{max} R_1, \quad (11a)$$

$$R_3 = \frac{G_{min} R_2}{G_{max} - G_{min}}, \quad (11b)$$

$$C_\alpha = \sqrt{\frac{G_{max}}{G_{min}}} \frac{\tau^\alpha}{R_2 + R_3}. \quad (11c)$$

Considering a low-pass filter of order $\alpha = 0.7$, $f_0 = 0.5 \text{ kHz}$, $G_{max} = 10$, $G_{min} = 1$, and assuming that $R_1 = 9 \text{ k}\Omega$, then the calculated values of the other elements of the filter are: $R_2 = 90 \text{ k}\Omega$, $R_3 = 10 \text{ k}\Omega$, and $C_\alpha = 112.7 \text{ nF} \cdot s^{-0.3}$.

The corresponding implementation of a fractional-order high-pass shelving filter is depicted in Fig. 2, with the realized transfer function being

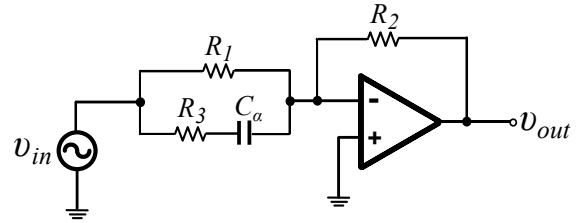


Fig. 2. Implementation of an op-amp based fractional-order high-pass shelving filter.

TABLE II
PASSIVE ELEMENTS VALUES OF THE NETWORK IN FIG. 3 FOR
APPROXIMATING THE FRACTIONAL-ORDER CAPACITORS IN FIGS. 1–2.

Element	Value	
	$C_\alpha = 112.7nF \cdot s^{-0.3}$	$C_\alpha = 1.13\mu F \cdot s^{-0.3}$
R_{F0}	562 Ω	56.2 Ω
R_{F1}	1.18 k Ω	118 Ω
R_{F2}	6.49k Ω	649 Ω
R_{F3}	33.2 k Ω	3.32 k Ω
R_{F4}	174 k Ω	17.4 k Ω
R_{F5}	1.54 M Ω	154 k Ω
C_{F1}	5.9 nF	59 nF
C_{F2}	11 nF	110 nF
C_{F3}	21.5 nF	215 nF
C_{F4}	41.2 nF	412 nF
C_{F5}	45.3 nF	453 nF

$$H(s) = -\frac{R_2 (R_1 + R_3) C_\alpha s^\alpha + 1}{R_1 R_3 C_\alpha s^\alpha + 1}, \quad (12)$$

and the associated design equations, derived from (7) and (12) provided by (13a)–(13c)

$$R_2 = G_{min} R_1, \quad (13a)$$

$$R_3 = \frac{R_2}{G_{max} - G_{min}}, \quad (13b)$$

$$C_\alpha = \sqrt{\frac{G_{max}}{G_{min}}} \frac{\tau^\alpha}{R_1 + R_3}. \quad (13c)$$

Following the same assumptions as in the case of the low-pass filter, the calculated values of the elements of the filters are the following: $R_2 = 9k\Omega$, $R_3 = 1k\Omega$, and $C_\alpha = 1.13\mu F \cdot s^{-0.3}$.

Due to the lack of commercial availability of fractional-order capacitors, their behavior can be approximated through the utilization of appropriately configured RC networks, such as the Foster type-I network in Fig. 3. Employing a 5th–

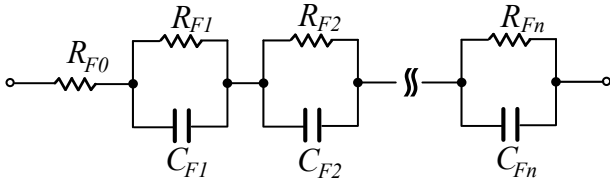


Fig. 3. Foster type-I RC network for approximating the behavior of fractional-order capacitors/impedances.

order Oustaloup approximation in the range $[10^2, 10^5]rad/s$, then the values of the elements of the network in Fig. 3 for substituting the fractional order capacitors in Figs. 1–2, calculated according to [12] and rounded to the E96 series defined in IEC 60063, are summarized in Table II.

Another possible solution for implementing the filters transfer functions is the employment of the general topology provided in Fig. 4, where the realized transfer function has the well-known form: $H(s) = -Z_2/Z_1$. The corresponding values of the impedances in the case of low-pass filters are

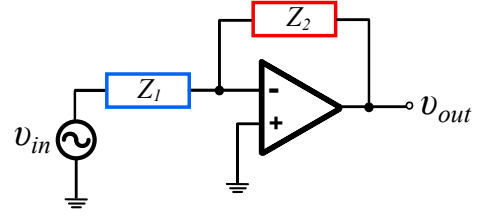


Fig. 4. Generalized topology for implementing the transfer functions of shelving filters.

TABLE III
PASSIVE ELEMENTS VALUES OF THE NETWORK IN FIG. 3 FOR
APPROXIMATING THE FRACTIONAL-ORDER IMPEDANCES IN FIG. 4

Element	Value	
	Z_2 in Fig. 4	Z_1 in Fig. 4
R_{F0}	9.53 k Ω	953 Ω
R_{F1}	976 Ω	97.6 Ω
R_{F2}	5.36k Ω	536 Ω
R_{F3}	24.9 k Ω	2.49 k Ω
R_{F4}	35.7 k Ω	3.57 k Ω
R_{F5}	9.76 k Ω	976 Ω
C_{F1}	7.3 nF	73.2 nF
C_{F2}	12.4 nF	124 nF
C_{F3}	20.5 nF	205 nF
C_{F4}	71.5 nF	715 nF
C_{F5}	1.65 μF	16.5 μF

given by (14a), while the corresponding ones in the case of high-pass filter are given by (14b)

$$Z_1 = R_1 \quad Z_2 = \frac{R_2 (R_3 C_\alpha s^\alpha + 1)}{(R_2 + R_3) C_\alpha s^\alpha + 1}, \quad (14a)$$

$$Z_1 = \frac{R_1 (R_3 C_\alpha s^\alpha + 1)}{(R_1 + R_3) C_\alpha s^\alpha + 1} \quad Z_2 = R_2. \quad (14b)$$

The approximation of the fractional-order impedance in (14a)–(14b) can be performed by expressing the Laplacian term s^α as a rational integer-order transfer function, derived using suitable approximation tools such as the Oustaloup, continued fraction expansion etc [12]. The resulting total impedance function has also the form of a ratio of integer-order polynomials, and it can be implemented using the RC network in Fig. 3.

Employing the 5th–order Oustaloup tool, for approximating the Laplacian term in the range $[10^2, 10^5]rad/s$, the values of passive elements for both low and high-pass filter functions are summarized in Table III. It is obvious that this solution offers reduced circuit complexity compared with the conventional procedure, where single fractional-order capacitors are substituted by RC networks.

IV. SIMULATION RESULTS

The performance of the filters based on the generalized topology in Fig. 4, will be evaluated using the OrCAD PSpice simulator and the corresponding model of the OP27 discrete component IC. The obtained magnitude and phase responses of the fractional-order filters in the acoustic band (20 Hz – 20 kHz) are depicted in Fig. 5 (solid lines), along with the corresponding ones derived by the Oustaloup approximation

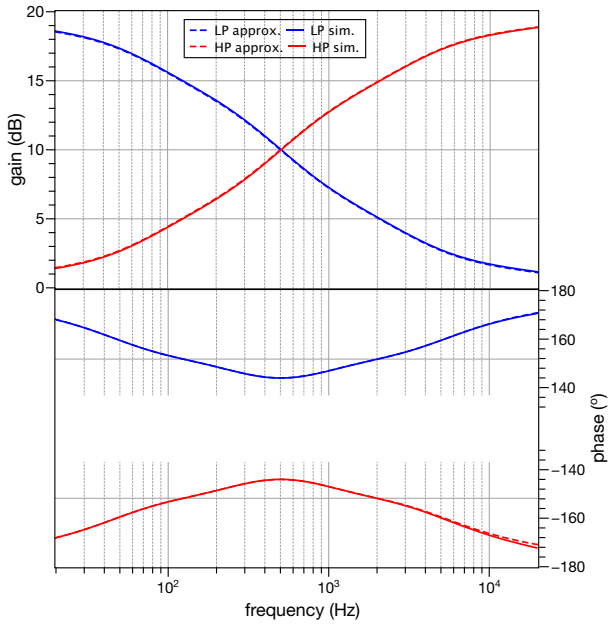


Fig. 5. Simulated gain and phase (shifted by 180°) responses of the shelving low-pass and high-pass filters, derived from the general topology in Fig. 4.

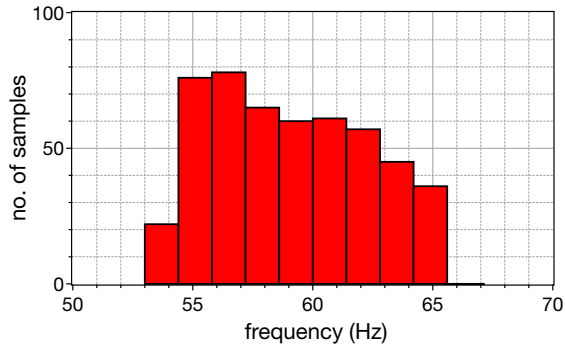


Fig. 6. Monte-Carlo analysis results of the low cut-off frequency of the fractional-order low-pass shelving filter.

of the transfer functions, marked by dashes. In the case of the low-pass filter, the simulated values of the low (f_L) and high (f_H) cut-off frequencies are 59.10Hz and 4.42kHz , while for the high-pass filter the corresponding values are 59.06Hz and 4.40kHz , with the theoretically predicted ones being 58.63Hz and 4.26kHz , respectively.

The sensitivity of the filters, with regards to the effect of passive components values tolerances is evaluated through the utilization of the Monte-Carlo analysis tool offered by the Advanced Analysis tool of the OrCAD PSpice suite for $N=500$ runs, and considering 10% random tolerances. The obtained statistical plots of the low-pass filter are demonstrated in Figs. 6–7, where the values of the standard deviation of the low and high characteristics frequencies $\{f_L, f_H\}$ are 3.2Hz and 0.2kHz . In the case of the high-pass filter, the corresponding results are 3.1Hz and 0.18kHz , respectively. As the nominal values are 58.63Hz and 4.26kHz , the proposed implementations offer reasonable sensitivity characteristics.

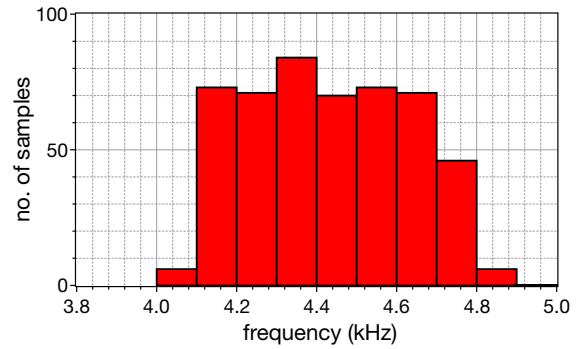


Fig. 7. Monte-Carlo analysis results of the high cut-off frequency of the fractional-order low-pass shelving filter.

V. CONCLUSIONS

The presented concept where, instead of substituting the fractional-order capacitors by suitable RC network, the whole synthetic impedance is substituted by a such network offers reduction of the passive component count and, also, provides design versatility. The performance characteristics of the resulted shelving filters structures, evaluated through the OrCAD PSpice suite, make them attractive candidates for employment in a wide variety of acoustic applications, where fine adjustment of the transition between the two bands is required.

REFERENCES

- [1] R. Izhaki, *Mixing audio: concepts, practices, and tools*. Routledge, 2017.
- [2] M. Holters and U. Zölzer, “Parametric higher-order shelving filters,” in *2006 14th European Signal Processing Conference*. IEEE, 2006, pp. 1–4.
- [3] A. Fernandez-Vazquez, R. Rosas-Romero, and J. Rodriguez-Asomoza, “A new method for designing flat shelving and peaking filters based on allpass filters,” in *17th International Conference on Electronics, Communications and Computers (CONIELECOMP’07)*. IEEE, 2007, pp. 10–10.
- [4] S. Sarkka and A. Huovilainen, “Accurate discretization of analog audio filters with application to parametric equalizer design,” *IEEE Transactions on Audio, Speech, and Language Processing*, vol. 19, no. 8, pp. 2486–2493, 2011.
- [5] V. Välimäki and J. D. Reiss, “All about audio equalization: Solutions and frontiers,” *Applied Sciences*, vol. 6, no. 5, p. 129, 2016.
- [6] G. A. Haidar, R. A. Z. Daou, and X. Moreau, “Synthesis of a fractional order audio boost filter,” in *2017 29th International Conference on Microelectronics (ICM)*. IEEE, 2017, pp. 1–5.
- [7] F. Schultz, N. Hahn, and S. Spors, “Shelving filter cascade with adjustable transition slope and bandwidth,” in *Audio Engineering Society Convention 148*. Audio Engineering Society, 2020.
- [8] L. Fierro, J. Rämö, V. Välimäki *et al.*, “Adaptive loudness compensation in music listening,” in *Sound and Music Computing Conference*, 2019.
- [9] G. Tsirimokou, C. Psychalinos, and A. Elwakil, *Design of CMOS analog integrated fractional-order circuits: applications in medicine and biology*. Springer, 2017.
- [10] S. Kapoulea, C. Psychalinos, and A. S. Elwakil, “Fractional-order shelving filter designs for acoustic applications,” in *2020 IEEE International Symposium on Circuits and Systems (ISCAS)*. IEEE, 2020, pp. 1–5.
- [11] S. Kapoulea, A. Yesil, C. Psychalinos, S. Minaei, A. S. Elwakil, and P. Bertsis, “Fractional-order and power-law shelving filters: Analysis and design examples,” *IEEE Access*, vol. 9, pp. 145 977–145 987, 2021.
- [12] G. Tsirimokou, “A systematic procedure for deriving RC networks of fractional-order elements emulators using Matlab,” *AEU-International Journal of Electronics and Communications*, vol. 78, pp. 7–14, 2017.